

Simulating pasta phases by molecular dynamics and cold atoms — Formation in supernovae and superfluid neutrons in neutron stars

Gentaro WATANABE^{1,2}

¹*Asia Pacific Center for Theoretical Physics (APCTP)
POSTECH, San 31, Hyoja-dong, Nam-gu, Pohang, Gyeongbuk 790-784, Korea*
²*RIKEN, 2-1 Hirosawa, Wako, Saitama 351-0198, Japan*

In dense stars such as collapsing cores of supernovae and neutron stars, nuclear “pasta” such as rod-like and slab-like nuclei are speculated to exist. However, whether or not they are actually formed in supernova cores is still unclear. Here we solve this problem by demonstrating that a lattice of rod-like nuclei is formed from a bcc lattice by compression. We also find that the formation process is triggered by an attractive force between nearest neighbor nuclei, which starts to act when their density profile overlaps, rather than the fission instability. We also discuss the connection between pasta phases in neutron star crusts and ultracold Fermi gases.

§1. Introduction

Collapse driven supernova explosion, an explosion in the death of a massive star, is one of the most dramatic phenomena in the universe and has been a long-standing mystery in astrophysics.¹⁾ One of the key ingredients to understand the mechanism of the supernova explosion is the study of matter in the core of supernovae.²⁾

State of matter in supernova cores also undergoes dramatic changes in the process of the collapse. Matter experiences an adiabatic compression, in which the density in the central region of the core increases from $\sim 10^9$ g cm⁻³ in the beginning of the collapse and finally reaches around the normal nuclear density $\sim 3 \times 10^{14}$ g cm⁻³ (corresponding to the number density of nucleons $\rho_0 = 0.165$ fm⁻³) just before the bounce. It is predicted that, in the final stage of the collapse, nuclei are rod-like or slab-like rather than (roughly) spherical in the central region of the core.^{3),4)} These non-spherical nuclei are collectively called nuclear “pasta”.

Recently, nuclear pasta attracts much attention of astrophysicists and nuclear physicists [see, e.g., Refs. 5), 6)] since it has been pointed out that the nuclear pasta would exist significant amount in supernova cores⁷⁾ and thus might have influences on the dynamics of supernova explosions.^{7)–9)} However, a fundamental problem of whether or not and how pasta phases are formed during the collapse is still unclear. In the present work,¹⁰⁾ we succeed in numerically simulating the formation of a triangular lattice of rod-like nuclei from a bcc lattice of spherical nuclei in collapsing cores and solve the above long-standing problem. In addition, we discover that the formation process is very different from a generally accepted scenario based on an instability with respect to nuclear fission. Our work provides a solid basis for understanding materials in supernova cores, which is indispensable for solving a long-standing problem of the mechanism of supernova explosions.

§2. Fission Instability?

In a generally accepted conjecture, based on the Bohr-Wheeler condition for vanishing the fission barrier derived for isolated nuclei, it is predicted that the formation of the pasta phases are triggered by the fission instability with respect to the quadrupolar deformation of spherical nuclei.¹¹⁾ The essential point of this prediction is that, at higher densities, the effect of the Coulomb repulsion between protons in nuclei, which tends to make a nucleus deform, becomes dominant over the effect of the surface tension of the nuclei, which favors a spherical nucleus. However, Refs. 12) and 13) have pointed out that the background electrons, which has been ignored in the above prediction, suppress the effect of the Coulomb repulsion between protons in nuclei and the fission barrier never vanishes in the relevant density region. These findings cast a doubt on the above conjecture based on the fission instability.

§3. Theoretical Framework

Since formation of the pasta phases is accompanied by dynamical and drastic changes of the nuclear structure, an *ab-initio* approach is called for. The quantum molecular dynamics (QMD),¹⁴⁾ which can properly incorporate the thermal fluctuations¹⁵⁾ and enables us to simulate large systems with $\sim 10^3$ nucleons or more,¹⁶⁾ is a suitable approach for the present purpose.

We use the QMD Hamiltonian of Ref. 17). In our simulations, we consider a system with protons, neutrons, and charge-neutralizing background electrons in a cubic box with periodic boundary condition. Here, we shall focus on the case of the proton fraction $x \simeq 0.39$ (total number of nucleons $N = 3328$ with 1312 protons and 2016 neutrons).

We simulate the compression of the bcc phase of spherical nuclei in the collapse [see Ref. 10) for detailed procedures]. Starting from $\rho = 0.15\rho_0$, we increase the density by changing the box size L (the particle positions are rescaled at the same time). Here the average rate of the compression is $\lesssim \mathcal{O}(10^{-6}) \rho_0/(\text{fm}/c)$ yielding the time scale of $\gtrsim 10^5 \text{ fm}/c$ to reach the typical density region of the phase with rod-like nuclei. This is much larger than the time scale of the change of nuclear shape and thus the dynamics observed in our simulation is determined by the intrinsic physical properties of the system. We perform adiabatic compression and isothermal compression at various temperatures [see Ref. 10) for details]. In all the cases, we observe the formation of rod-like nuclei; here we show a typical example in which we obtain a clear lattice structure of the rod-like nuclei.

§4. Results

Figure 1 shows the snapshots of the formation process of the pasta phase in adiabatic compression. Here, we start from initial condition at $\rho = 0.15\rho_0$ and $T = 0.25 \text{ MeV}$ ($t = 0 \text{ fm}/c$). At $\rho \simeq 0.243\rho_0$ [Fig. 1(c)], the first pair of two nearest-neighbor nuclei start to touch and fuse (dotted circle), and then form an elongated nucleus [see, e.g., Fig. 1(d)]. After multiple pairs of nuclei become such elongated

nuclei, we observe zigzag structure as shown in Fig. 1(d). Then these elongated nuclei stick together [see Figs. 1(e) and (f)], and all the nuclei fuse to form rod-like nuclei as shown in Fig. 1(g). Finally, we obtain a triangular lattice of rod-like nuclei after relaxation [Figs. 1(h-1) and (h-2)].

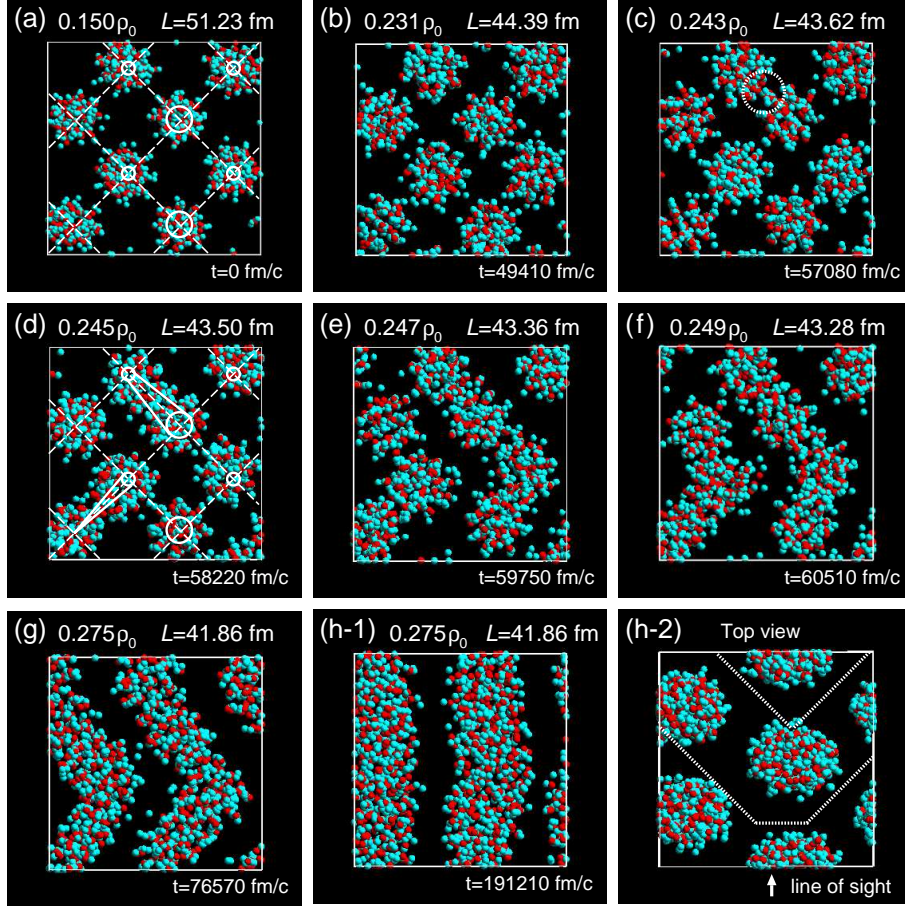


Fig. 1. (Color online) Snapshots of the transition process from the bcc lattice of spherical nuclei to the pasta phase with rod-like nuclei. The red particles show protons and the green ones neutrons. In panels (a)-(g) and (h-1), nucleons in a limited region relevant for the two rod-like nuclei in the final state (h) [surrounded by the dotted lines in panel (h-2)] are shown for visibility. The vertices of the dashed lines in panels (a) and (d) show the equilibrium positions of nuclei in the bcc lattice and their positions in the direction of the line of sight are indicated by the size of the circles: vertices with a large circle, with a small circle, and those without a circle are in the first, second, and third lattice plane, respectively. The solid lines in panel (d) represent the direction of the two elongated nuclei: they take zigzag configuration. The box sizes are rescaled to be equal in the figures. This figure is taken from Ref. 10).

Note that before nuclei deform to be elongated due to the fission instability, they stick together keeping their spherical shape [see Fig. 1(c)]. Besides, in the middle of the transition process, pair of spherical nuclei get closer to fuse in a way such that the resulting elongated nuclei take a zigzag configuration and they further connect

to form wavy rod-like nuclei. This feature is observed in all the other cases in which we obtain a clear lattice structure of rod-like nuclei, and the above scenario of the transition process is qualitatively the same also for those cases. It is very different from a generally accepted picture that all the nuclei elongate in the same direction along the global axis of the resulting rod-like nuclei and they join up to form straight rod-like nuclei.¹¹⁾

Instead of such a scenario, we have shown that the pasta phases are formed in the following process [see Ref. 10) for details]. When nearest neighbor nuclei are so close that the tails of their density profile overlap with each other, net attractive interaction between these nuclei starts to act. This internuclear attraction leads to the spontaneous breaking of the bcc lattice and triggers the formation of the pasta phases.

§5. Simulating Pasta Phases by Ultracold Fermi Gases

In the remaining part of this article, we shall discuss the connection between the pasta phases and the ultracold atomic Fermi gases. Pasta phases can exist also in crusts of neutron stars. There, pasta nuclei are immersed in background electrons and a gas of dripped neutrons, which is regarded to be in a superfluid state.

It has been pointed out that the low density neutron matter shows the same universal property as unitary Fermi gases provided that the interparticle separation r_s between neutrons is much smaller than the absolute value of the scattering length $a \simeq -18.5$ fm and is much larger than the effective range $r_e \simeq 2.7$ fm^{18),19)} [see also Refs. 20)–22)]. Here, “universal” means that properties do not depend on details of the nuclear potential.

In dripped neutron gas in the pasta phases, the density is $\rho_n = k_F^3/(3\pi^2) \gtrsim 0.05$ fm⁻³ and thus the interparticle separation $r_s \gtrsim 1.7$ fm is comparable to r_e (here, k_F is the Fermi wave vector of the ideal Fermi gas with the same density). However, Schwenk and Pethick^{22),23)} have shown that in such a region of $k_F r_e \sim 1$, corrections from the universality in the equation of state is accurately described within the effective range expansion and no further details of nuclear forces are not needed. The energy per particle E/N can be expressed in the same form as the universal case but with a r_e -dependent factor $\xi(k_F r_e)$: $E/N = \xi(k_F r_e) (3/5)E_F$ with $E_F \equiv \hbar^2 k_F^2/2m$ and m being the fermion (neutron, in the present case) mass. This means that the dripped neutron gas in the pasta phases can be simulated by cold atomic Fermi gases with a narrow Feshbach resonance. At qualitative level, we can also expect that unitary Fermi gases would provide a suggestive guidance for exploring interesting physical effects related to the dripped superfluid neutrons in the pasta phases.

In Refs. 24) and 25), we have studied superfluid unitary Fermi gases in a one-dimensional (1D) periodic potential $V_{\text{ext}}(z) = sE_R \sin^2(q_B z)$, where s is the laser intensity, $E_R = \hbar^2 q_B^2/2m$ is the recoil energy, $q_B = \pi/d$ is the Bragg wave vector, and d is the lattice constant. This setup resembles superfluid neutrons in the pasta phase with slab-like nuclei, where $\rho_n \simeq 0.5\rho_0 \simeq 0.08$ fm⁻³ and $d \simeq 15 - 20$ fm and thus $E_F/E_R = (k_F/q_B)^2 \sim 40 - 70$. Since the difference $\delta\Delta$ in the pairing field Δ

between inside and outside the nuclei is $O(1)$ MeV, $s \sim |\delta\Delta|/E_R$ is estimated to be $O(1)$.

In Fig. 2, we show the incompressibility $\kappa^{-1} = n\partial_n^2 e$ and the effective mass $m^* = n(\partial_P^2 e)^{-1}$ of the unitary Fermi gas. Here $e = e(n, P)$ is the energy density averaged over the unit cell as a function of the average (coarse-grained) density n and the quasimomentum P of the superflow in the z direction.

The rapid reduction of κ^{-1} with decreasing E_F/E_R at small E_F/E_R is due to the formation of bosonic molecules induced by the periodic potential. Maximum of κ^{-1} and m^* around $E_F/E_R \sim 1$ is the effect of the energy band gap. Since the tunneling rate through the barriers, which relates to m^* , depends on the barrier height exponentially, m^* increases drastically for larger s . The enhancement of m^* has been found also in dripped neutron gas in the crust of neutron stars.²⁶⁾

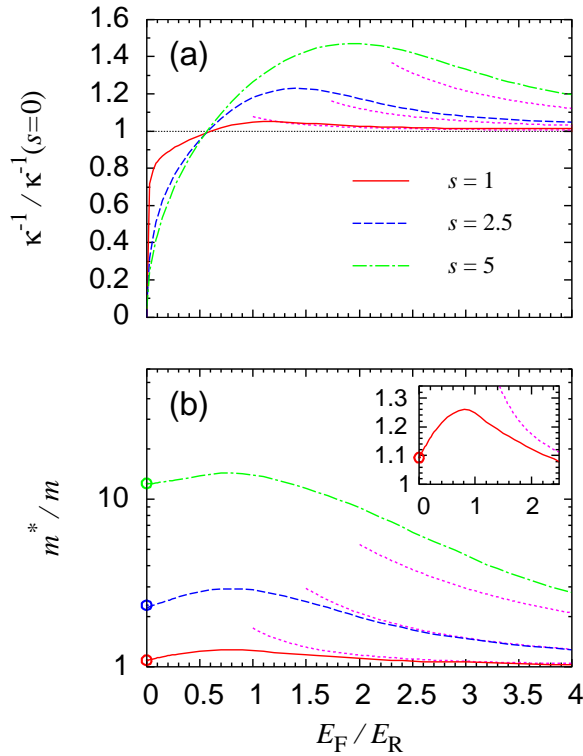


Fig. 2. (Color online) Inverse compressibility κ^{-1} , and effective mass m^* of the unitary Fermi gas for $s = 1$ (red), 2.5 (blue), and 5 (green). The solid, dashed, and dash-dotted lines show the results obtained by the Bogoliubov-de Gennes (BdG) equations. The dotted lines show the asymptotic expressions [Eqs. (5.1) and (5.2) with $r_e = 0$ and $\partial_n \xi = 0$] obtained by the hydrodynamic theory. The $s = 1$ results for m^* are also shown in the inset in the linear scale. Adapted from Fig. (1) in Ref. 24).

Taking account of the density dependence of ξ in the case of the large effective range, we derive κ^{-1} and m^* for $sE_R/E_F \ll 1$ using the equation of state, $E/N = (3/5)\xi E_F$, within the hydrodynamic theory. In the relevant region of $k_F r_e \gtrsim 3$, $\partial_n^2 \xi$ is negligible, and keeping up to the first order of $\partial_n \xi$ ($n\xi^{-1}\partial_n \xi \lesssim 0.1$ in this region²³⁾),

we obtain

$$\kappa^{-1} \simeq \frac{2}{3} \xi E_F \left\{ 1 + \frac{1}{32} \xi^{-2} \left(\frac{s E_R}{E_F} \right)^2 + 3n \xi^{-1} \partial_n \xi \left[1 + \frac{1}{32} \left(\frac{s E_R}{E_F} \right)^2 \right] \right\}, \quad (5.1)$$

and

$$\frac{m^*}{m} \simeq 1 + \frac{9}{32} \xi^{-2} \left(\frac{s E_R}{E_F} \right)^2. \quad (5.2)$$

Since ξ is a monotonically increasing function of $k_F r_e$,²³⁾ m^* for non-zero r_e is smaller than that of unitary Fermi gases.

Acknowledgements

Works reported in this paper have been done in collaborations with H. Sonoda, K. Sato, K. Yasuoka, T. Ebisuzaki, F. Dalfovo, G. Orso, F. Piazza, L. P. Pitaevskii, and S. Stringari. We used MDGRAPE-2 and -3 of the RIKEN Super Combined Cluster System, WIGLAF at the University of Trento, and BEN at ECT*. We were supported by the JSPS, by the MEXT through Grant No. 19104006, by EuroQUAM-FerMix, by MiUR, by CNR, and by the EC Sixth Framework Programme.

References

- 1) S. A. Colgate and R. H. White, *Astrophys. J.* **143** (1966), 626.
- 2) H. A. Bethe, *Rev. Mod. Phys.* **62** (1990), 801.
- 3) D. G. Ravenhall, C. J. Pethick, and J. R. Wilson, *Phys. Rev. Lett.* **50** (1983), 2066.
- 4) M. Hashimoto, H. Seki, and M. Yamada, *Prog. Theor. Phys.* **71** (1984), 320.
- 5) K. Oyamatsu, contribution to this volume.
- 6) K. Nakazato, contribution to this volume.
K. Nakazato, K. Oyamatsu, and S. Yamada, *Phys. Rev. Lett.* **103** (2009), 132501.
- 7) H. Sonoda *et al.*, *Phys. Rev. C* **75** (2007), 042801(R).
- 8) G. Watanabe, K. Iida, and K. Sato, *Nucl. Phys.* **A687** (2001), 512.
- 9) C. J. Horowitz, M. A. Pérez-García, and J. Piekarewicz, *Phys. Rev. C* **69** (2004), 045804.
C. J. Horowitz *et al.*, *ibid.* **70** (2004), 065806.
- 10) G. Watanabe *et al.*, *Phys. Rev. Lett.* **103** (2009), 121101.
- 11) C. J. Pethick and D. G. Ravenhall, *Annu. Rev. Nucl. Part. Sci.* **45** (1995) 429.
- 12) S. Brandt, Master thesis, Copenhagen Univ. (1985).
- 13) T. J. Bürvenich, I. N. Mishustin, and W. Greiner, *Phys. Rev. C* **76** (2007), 034310.
- 14) J. Aichelin, *Phys. Rep.* **202** (1991), 233.
- 15) G. Watanabe *et al.*, *Phys. Rev. C* **69** (2004), 055805.
H. Sonoda *et al.*, *Phys. Rev. C* **77** (2008), 035806.
- 16) G. Watanabe *et al.*, *Phys. Rev. C* **66** (2002), 012801(R); *Phys. Rev. C* **68** (2003), 035806;
Phys. Rev. Lett. **94** (2005), 031101.
- 17) T. Maruyama *et al.*, *Phys. Rev. C* **57** (1998), 655.
- 18) G. F. Bertsch, in the announcement of the Tenth International Conference on Recent Progress in Many-Body Theories, (1999) unpublished.
- 19) G. A. Baker, Jr., *Phys. Rev. C* **60** (1999), 054311.
- 20) A. Gezerlis and J. Carlson, *Phys. Rev. C* **77** (2008), 032801(R).
- 21) T. Abe and R. Seki, *Phys. Rev. C* **79** (2009), 054003.
- 22) C. J. Pethick, contribution to this volume.
- 23) A. Schwenk and C. J. Pethick, *Phys. Rev. Lett.* **95** (2005), 160401.
- 24) G. Watanabe *et al.*, *Phys. Rev. A* **78** (2008), 063619.
- 25) G. Watanabe *et al.*, *Phys. Rev. A* **80** (2009), 053602.
- 26) N. Chamel, *Nucl. Phys. A* **773** (2006), 263.